NUMERICAL METHODS IN UNDERWATER ACOUSTICS - SOUND PROPAGATION AND BACKSCATTERING

BODO NOLTE[1,2], JAN EHRLICH[2], HANS-GÜNTER HOFMANN[2], INGO SCHÄFER[2], ALEXANDRA SCHÄFKE[2], ARNE STOLTENBERG[2], RALF BURGSCHWEIGER[3]

[1] Embassy of the Federal Republic of Germany in Poland, Jazdów 12, 00-467 Warsaw
mil-3@wars.auswaertiges-amt.de

[2]Bundeswehr Technical Centre for Ships and Naval Weapons, Maritime Technology and Research, Berliner Straße 115, 24340 Eckernförde, Germany

[3] Beuth University for Applied Sciences, Luxemburger Straße 10, 13353 Berlin

This report summarizes an overview given at the XXXII Symposium on Hydroacoustics (SHA 2015) over several modeling techniques that are used in the context of military applications at the Research Department FWG of the German Bundeswehr Technical Centre for Ships and Naval Weapons, Maritime Technology and Research (WTD 71). For the modeling and understanding of sound propagation, a physical model consisting of a tank for the scaled measurements and the corresponding numerical simulation is presented. The basic formalism of the stochastic ray tracing of the German Navy sonar simulation MOCASSIN is explained and compared to traditional deterministic ray tracing, and this includes comparisons with measurements. Strategies for the approximate calculation of the sonar target strength of large underwater objects with the use of boundary element methods, fast multipole methods as well as a ray-based algorithm, are all presented here and the results of the calculations of several test objects are shown.

INTRODUCTION

One application in the broad field of hydroacoustics is the search for underwater objects with the use of sonar. Specific military interest lies in the detection of submarines in varying conditions. Shallow water regions pose particular problems, for example, places such as the Baltic Sea or the North Sea, where sound propagation can be very complex, depending on the environmental conditions. In order to perform this task successfully, one has to be able to predict the outcome of this search using simulations, whilst taking into account the current

environmental conditions. The simulation process can be roughly divided into two parts: the propagation of sound from the sonar to the target and back again, and the scattering of sound away from the target in question. Both problems can be treated with simulations but the mathematical methods involved are different. Here, three kinds of simulation are presented that have been developed at WTD 71: a physical modeling of sound propagation with both a scaled tank model with a corresponding numerical model, a stochastic ray tracing approach in use with the German Navy Sonar Simulation model MOCASSIN, as well as techniques providing the reliable and fast calculation of the sonar target strength of submerged objects.

1. PHYSICAL AND NUMERICAL SIMULATIONS OF SOUND PROPAGATION

In the research project “Virtual Ocean”, the development and validation of a phase-exact sound propagation model for modern underwater applications are supported by high-precision measurements performed in water-tank experiments.

The newly developed PESSim (parabolic equation sound simulation) model is based on an approximation of the wave equation as a parabolic differential equation and allows a phase-exact calculation of the sound pressure field. The model can handle depth- and range-dependent properties of water column and sea bottom. It also particularly takes any occurring pressure and sheer waves found at the sea bottom into account, as well as any arbitrary layers in water column and bottom, and additionally includes range-dependent bathymetry.

Sound propagation in water is influenced by a variety of environmental parameters, such as sound speed profiles in the water column, surface waves, bathymetry and the geo-acoustical properties of the sea bottom. Therefore a real ocean, with its multitude of difficult-to-measure, strongly variable and poorly reproducible environmental parameters, is too complex to allow for a detailed validation of a sound propagation model in sea experiments.

For this reason, in parallel with the development of the numerical model, a scaled (1:100), simplified model of an ocean was tested in a tank experiment. This type of experiment places high demands on the precision of the measurements. To achieve this required precision, a frame incorporating high-precision linear actuators was constructed, and upon which the transmitter is firmly fixed, whereas the receiving hydrophone can be positioned in all three spatial dimensions within an accuracy of 0.2mm (Fig. 1).

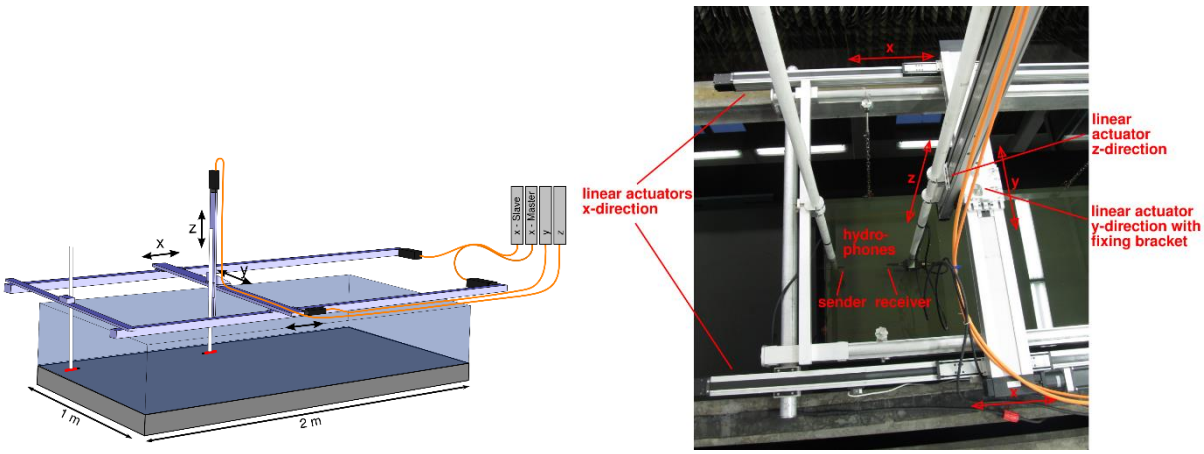

Fig.1. Left: Sketch of the tank experiment, Right: Highly precise positioning of transmitter and receiver.

In the base scenario, a horizontally mounted slab of homogeneous PVC serves as the sea bottom. Measurement data from the physical simulations in the water tank experiment are used to validate numerical simulations and the corresponding sound propagation model.

The interaction of physical and numerical simulations permits the selective study of the effects of the individual parameters and thus facilitates reliable predictions, even in complex, realistic scenarios. The complexity of both the simulations (numerical and physical) can be gradually increased in a controlled manner for each single parameter. This ensures that the numerical model correctly describes the influence of each relevant parameter in the sound propagation.

Figure 2 shows a comparison of measurement data from the tank experiment (physical simulation) with results from the numerical simulation for the base scenario at 185 kHz.

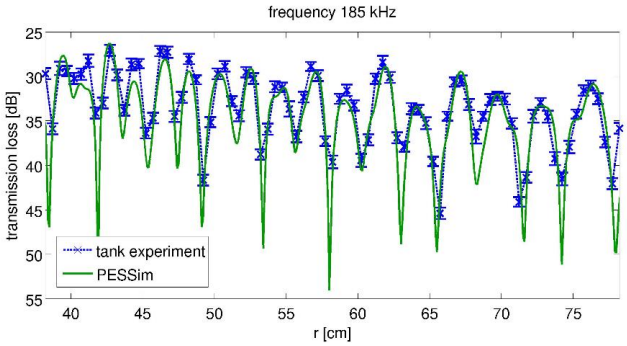

Fig. 2. Comparison of measurement data from the tank experiment with results from the numerical simulation.

The first simple variations of the base scenario may include the inclination of the PVC slab or the addition of a sediment layer. More complex bathymetries, surface waves and the suitable layering of the water column will all follow later. Eventually, the sound propagation model will have to prove itself under real conditions in sea trials. The extent of the required sea trials and the resulting costs can, however, be reduced considerably, through the interaction of numerical and physical simulations, as was described above.

2. LONG RANGE PROPAGATION WITH STOCHASTIC RAY TRACING

2.1 Ray tracing approach

For moderate to high frequencies and long ranges, ray tracing formalism is a common and advantageous approach. The Helmholtz equation is solved by approximating the pressure *p(r)* as ray series

$$p(\vec{r}) = e^{i\omega\tau(\vec{r})} \sum_{j=0}^{\infty} \frac{A_j(\vec{r})}{(i\omega)^j} \tag{1}$$

After inserting this expression into the Helmholtz equation and sorting the resulting terms according to powers of ω,one obtains, in zeroth order, eikonal equation (2), which defines the rays, as well as in first order transport equation (3), which can be used in the calculation of pressure amplitude.

$$|\nabla\tau|^2 = \frac{1}{c^2(\vec{r})} \tag{2}$$

$$2\nabla\tau\cdot\nabla A_0+(\nabla^2\tau)A_0 \;=\; 0 \tag{3}$$

The eikonal equation can be transformed into a set of ordinary differential equations with the help of the two auxiliary parameters ξ und ζ

$$\begin{aligned}\frac{dx}{ds}&=c\,\xi(s) \quad , \qquad \frac{d\xi}{ds}=\frac{1}{c^2}\frac{dc}{dx}\\ \frac{dz}{ds}&=c\,\zeta(s) \quad , \qquad \frac{d\zeta}{ds}=\frac{1}{c^2}\frac{dc}{dz}\end{aligned} \tag{4}$$

This system of differential equations can be solved using standard methods such as the Euler method, as long as it has suitable starting values. One solution is presented in Equation (5), where the angle θ parametrizes the starting direction of the respective ray.

$$\begin{aligned}x(0)&=x_s \quad , \qquad \xi(0)=\frac{\cos\theta}{c(x_s,z_s)}\\ z(0)&=z_s \quad , \qquad \zeta(0)=\frac{\sin\theta}{c(x_s,z_s)}\end{aligned} \tag{5}$$

2.2 Stochastic ray tracing

For the simulation of long ranges, for example those present in submarine hunting applications, the governing parameters, such as the sound speed profile in the water column are only partly known, and may change over the distance of interest. In order to mimic this uncertainty, the concept of stochastic ray tracing may be used. The approach described below is implemented in the sonar prediction model MOCASSIN used by the German Navy. The acronym MOCASSIN stands for “Monte Carlo Schall-Strahlen Intensitäten”, which can be translated as ‘Monte Carlo Sound Ray Intensities’.

The model was developed (at the former Federal Armed Forces Research Institute for Underwater Acoustics and Marine Geophysics (FWG), now part of WTD 71), for active sonars in shallow waters with highly variable sound speed conditions and poor knowledge on the input data [1,2,3]. The variability is of a stochastic nature. This may happen to be sufficiently strong to influence the average sound pressure level and cause deviations from the values of the sound pressure level expected within a non-variable sound speed structure. This is especially true in shallow waters, where stochastic variations can be large compared to the relevant distances.

The main feature that sets MOCASSIN apart from other propagation models is the stochastic raytracing approach. This method uses a Monte Carlo approach for the stochastic change of ray directions and was found to be a very effective way of accommodating the acoustic forward scattering caused by variations in the sound speed in the water column. In line with the incoherent transmission loss data from the experiments, with the model's stochastic approach and its operational conditions and needs, the model calculates incoherent TL alone, and requires the specification of only one sound speed profile.

The propagation of underwater sound is computed in an optical or geometric acoustic approximation of the wave equation, which is better known as raytracing. This implies that acoustic wave length λ is small when compared to any other structure length L of importance when it comes to propagation. The most dominating structure length is evidently water depth *H*, thus, it is essential that $\lambda << H$. This creates no real restrictions for active sonars used in submarine hunting due to the fact that the lowest frequencies used are in the lower kHz

region, with wave lengths smaller than about 1 meter, allowing for water depths as shallow as 30m. In a case of a depth dependent sound speed profile c(z), the condition to be met is

$$\frac{\lambda}{c}\left|\frac{dc(z)}{dz}\right| << 1\ , \tag{6}$$

which means the sound speed variation should be small over the wavelength.

The vertical sound speed profile *c(z)* is approximated by linear segments, so that horizontal layers of constant sound speed gradients are formed. This allows for extremely effective numerical raytracing equations in which the ray paths are either straight lines (*dc /dz* = 0) or the arcs of a circle (*dc/dz*≠ 0). The calculation domain is divided into rectangles. The corners of the rectangles are defined in *z* by the points at which the linear sound speed segment start and end, and within range of the points at which linear segments of the bathymetry start and end. For large parts with constant bathymetry, a partition in range is chosen in a such a way that the aspect ratios of the calculation rectangles are not overly large.

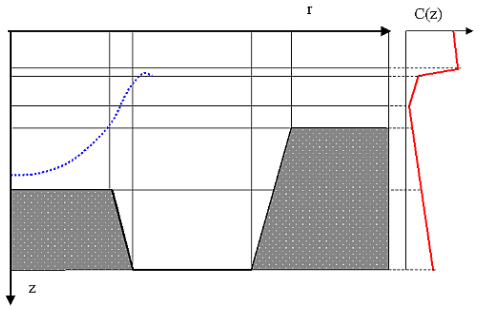

Fig.3. Schematic drawing of the calculation boxes from MOCASSIN defined by bathymetry and the linearized sound speed profile (right). The blue dotted line on the left shows the resulting ray.

The input sound speed profile should be sufficiently sampled, so that the fine structure, which is important for the highest frequency considered, is included. However, a locally measured vertical fine structure is only effective if it is persistent over a sufficiently large horizontal distance. If this is not the case, propagation may be erroneously dominated by a local feature. If necessary, a linearization process will reduce the number of points to an appropriate value, in order to be able to continue further calculations.

In some ocean areas, such as the Baltic Sea or Skagerrak, sound speed stratification is highly variable with range, over distances which are short in relation to propagation distances, which leads to horizontal sound speed gradients, for example, the thermocline may frequently change depth, while the main features of the vertical sound speed profiles remain conserved.

In these, and similar cases, the horizontal sound speed variability may often be described stochastically, that is to say that the variation may be assumed to occur randomly. The acoustic effect is that additional losses (leakage) from sound channels will occur or – *vice versa* – acoustic energy may be trapped in the sound channels. To model this effect, a diffusion approximation is assumed in which the diffusion constant *D* has been made dependent on the sound speed profile *c(z)*

$$D(z) = D_0\left(1 + g_0\left|\frac{dc(z)}{dz}\right|\right)^2 \tag{7}$$

D_0 is an empirical input quantity in the range of $10^{-10} \le D_0 \le 10^{-6}$ and g_0 is a scale factor with a numerical value one second. This assumes that the angular deviation $\Delta\phi$ of the rays' propagation angle from the deterministic conditions at the end of the layer is given by a Gaussian probability density for $\Delta\phi$, with

$$\overline{\Delta\phi} = 0 \quad , \qquad \sigma^2 = \overline{\Delta\phi^2} = 2\,D\,S \ ,$$

where S is the path length in that particular layer. The angular change is actually not applied at each layer boundary, but is accumulated over several the layers i, for a path length S_{sum}

$$S_{sum} = \sum S_i \qquad \text{and} \quad \sigma^2 = \sum S_i \, D_i(z) \tag{8}$$

and is applied in the range interval $DX_{STC} \leq S_{sum} \leq 2\,DX_{STC}$. This provides a certain randomizing of the locations where angular changes are applied. For meaningful statistical results, many events should occur over the total propagation range ($DX_{STC} << max.range$) and, for the diffusion approximation to hold, the angular change should be small (i.e. $\sigma^2 = 2\,D\,S << 1$). On the other hand, for computational efficiency, DX_{STC} should be large. The empirical compromise for the value DX_{STC} in meters is

$$DX_{STC} = \max\left(1000, \min\left(200\sqrt[3]{d_w}, max.range/20\right)\right) , \tag{9}$$

where the dimensionless number d_w is the value of the water depth in meters. In depths greater than 1500m, the sound speed structure is assumed to be invariant and no stochastic angular changes of the propagation angle are applied, i.e. $D\,(z \geq 1500\ \text{m}) = 0$.

Numerical values for the diffusion constant D_0 were empirically determined by the modelling of various environments. The following quantities are recommended:

$$D_0 \begin{cases} \leq 10^{-9} & \text{quasi deterministic (no variability)} \\ = 10^{-8} & \text{low variability (the North Sea and most areas)} \\ = 10^{-7} & \text{high variability (the Baltic, Skagerrak)} \end{cases}$$

2.3 Transmission loss computation

In contrast to deep water raytracing models, which compute the intensity at one particular point in depth and range through ray divergence methods, this model accumulates the intensity of rays penetrating a receiver window of vertical size Δ, at depth z, and range r. A maximum of 100 sample points in a range is allowed, as well as a maximum of 30 consecutive vertical receiver windows, spanning the depth range from z_0 to $z_{max} = z_0 + n\Delta$, with $1 \leq n \leq 30$.

Note that the loss is an incoherent average over depth interval Δ and insufficient values of Δ will result in rapidly fluctuating loss values due to insufficient ray statistics in the receiver window, as this is no eigenray solution. In order to give meaningful results, a large number of rays is required, usually somewhere in the order of several thousands. Thanks to the simple ray calculation process using stepwise linear sound speed profiles, the overall calculation is still very fast.

The standard vertical source characteristic is modeled by a parabola. The energy radiated decreases with angle ϕ:

$$E(\phi) = 1 - 2\left(\frac{\phi - \phi_t}{\phi_0}\right)^2 , \qquad |\phi - \phi_t| \leq \frac{\phi_0}{\sqrt{2}} \ , \tag{10}$$

where ϕ_t is the tilt angle against the horizontal and ϕ_0 is the opening angle between the two 3 dB points. A single ray represents the intensity in the angular interval $\Delta\phi = \sqrt{2}\phi_0 / N$, which is sufficiently approximated by $I(\phi) = E(\phi)\cdot\Delta\phi$ as long as the number of rays N in the above

interval is adequately large. Numerical realisation assumes a constant intensity for all rays and attributes larger angular intervals to a single ray in accordance with this energy distribution.

The use of such an approximated beam profile is allowed for long range propagation with relatively realistic sonar beams in shallow water, where far-field intensity is dominated by rays with small inclinations. Rays with steeper angles are not take into account because they rapidly lose energy through their numerous reflections onto the seafloor and the surface.

This type of ray-tracing approach in which the intensity between two adjacent rays is not interpolated in space, is mathematically exact only within the parameters of an infinite number of rays. However, for most practical applications, a few thousand rays will constitute a sufficient approximation. Deviations in the computed loss occur if different numbers of rays or different sequences of random numbers are used. These deviations are generally insignificant at high intensity regions and will be predominantly noticeable at large intensity gradients or in low intensity (high loss) areas into which the intensity has been carried through by only a few rays. Smoothing the propagation loss curves with splines will reduce these differences.

2.4 Comparison with measurements

Over the years, several comparisons between measured and modeled transmission loss data have been made [4,5,6]. To give one example, the recordings of transmission loss made in 2006 and 2007 in the Baltic Sea are compared with simulations with stochastic ray tracing [7]. The measurements were conducted with a receiving vertical array on a moored ship (FS Planet) and a transmitter that was towed by a second ship (S/V Ocean Surveyor) along a track 55 km away from the receiver. Figure 5 shows the measured and modeled transmission loss values for two different runs (A05 from 2006, left and A28 from 2007) and the two different hydrophone depths. In all cases, the stochastic calculations are in far better accordance with the measured values than with the deterministic calculations.

For both trials, the observed oceanographic conditions were typical for the Baltic Sea's summer conditions, but were not identical. The recorded temperature, salinity and resulting sound speed profiles are shown in Figure 4.During the 2006 trial, there was a very sharp thermocline and the sound speed minimum was about 1427m/s at a depth of between 30m and 35 m. During the 2007 trial, the sound speed minimum was only about 1435m/s, roughly 10m deeper, and the thermocline change was more gradual.

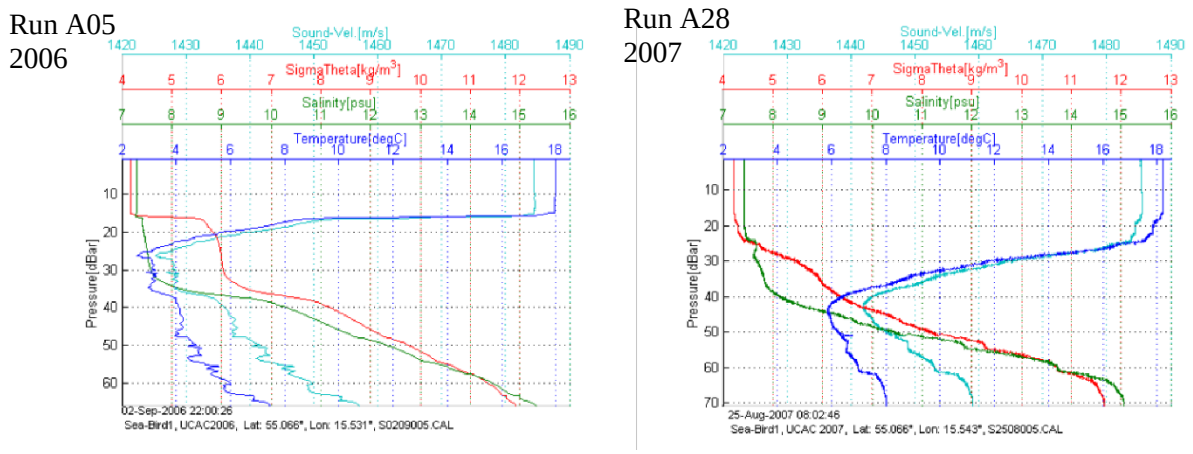

Fig.4. Temperature and salinity measurements and resulting sound speed profiles for the A05 run of the 2006 trial (left) and the A28 run of the 2007 trial.

Simulations with MOCASSINwere performed for several runs in 2006 and 2007 using four different frequencies. The modeled TL curves for Run A05 (2006) show decent accordance with the measurements for 3400 Hz (Fig. 5, upper picture) for the stochastic calculations. It is emphasized here that a deterministic model would not be able to properly predict the TL outside the sound channel with only one sound-speed profile given as the input. For a hydrophone depth of 35m, the receiver was within the sound channel and the transmission was somewhat low. At a hydrophone depth of 14m, the hydrophone was outside the sound channel and, therefore the transmission loss was significantly greater.

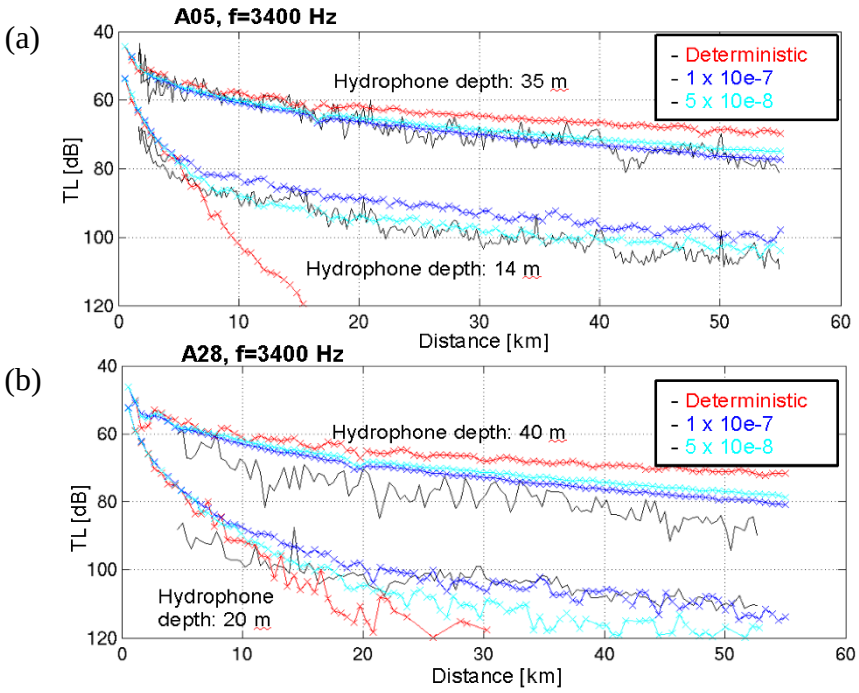

Fig.5. Measured (black) and modeled transmission loss for different hydrophone depths for the A05 run of the 2006 trial (a) and the A28 run of the 2007 trial (b). The modeled transmission loss curves vary in the diffusion constant D0, from D_0=10^{-9}zero (quasi deterministic, red) to D_0=$5{\cdot}10^{-8}$ (cyan) and D_0=10^{-7} (blue).

For run A28 from 2007, the same level of accordance could not be reached, although the measurements were conducted at the same site. Nevertheless, the results with the diffusion constant D_0 of 10^{-7}, the general recommendation for the Baltic Sea, a high variability region, gives the best results. It might be necessary to use a frequency and position-dependent diffusion function rather than a constant.

3. NUMERICAL METHODS TO DETERMINE SCATTERED PRESSURE OF UNDERWATER OBJECTS

The most applied methods for the prediction of the scattered pressure of underwater objects in the far-field may be grouped into four different basic methods: the Boundary Element Method (BEM), the Finite Element Method (FEM), approximate methods and raytracing methods.

3.1 Boundary Element Method (BEM)

This method only requires the three-dimensional modeled surface of the objects of interest, which is represented by a discretization into triangular and/or quadrilateral elements. In general, this leads to a complex system of equations that can be solved by different kinds of solvers:

- Direct solver (matrix based): usable for bi- and monostatic calculations (element limit approx. 200k)
- Iterative solver (matrix based): Usable for bistatic calculations (element limit approx. 300k)
- Iterative solver combined with the fast multipole method (MLFMM): Usable for bistatic rigid calculations (element limit approx. 5M)

3.2 Finite Element Method (FEM)

This method requires a three-dimensional model of full volume using so-called finite elements, which may have four or more different nodes. This method is often not feasible for large objects or calculations in the far-field because the number of volume elements required, which results in large, sparse matrices, cannot be handled by standard workstations.

One practical alternative is the use of two-dimensional FEM calculations with simple rotational symmetric objects for rigid and coupled cases.

3.3 Approximate (PWA, KIA) and raytracing based methods (BEAM)

These methods do not require large equation systems, but are able to calculate usable, approximate solutions within reasonable times, mostly within the mid and high frequency range. Depending on the method used, they are usable for rigid (PWA, KIA) and coupled calculations with inner structures (BEAM).

3.4 Acoustic backscattering

The acoustic sound backscattering p_{scat} of the surface Γ of the object can be calculated by means of the Kirchhoff-Helmholtz integral (Eq. 11), at a known pressure and velocity field (resulting from one of the methods mentioned above):

$$p_{scat} = \int_{\Gamma} \left[g \frac{\partial p}{\partial n} - p \frac{\partial g}{\partial n} \right] d\Gamma, \; TS = 20 \log \left(\frac{p_{scat}}{p_{inc}} \right) \tag{11}$$

with

g fundamental solution of the Helmholtz equation
p_{inc} incident pressure
TS target strength (normalized pressure level at a distance of 1m from the center)

Using a full coupled boundary element calculation, the unknown pressure and velocity values maybe determined on the surface of the object and, at that juncture, in a post-processing step, and additionally from the backscattered sound pressure at any point in the far-field.

3.5 Results for different kinds of objects and methods

3.5.1 Icosahedron (bistatic)

Using an icosahedron (113,940 elements, diameter ≈ 0.33 m, 20 triple mirrors, Fig. 6, details see [8]), the results are compared with a BEM solution. The target strength is calculated at a frequency of f = 100 kHz on an observation surface (spherical segment, placed centered over one of the mirrors, 8,457 elements, 4,360 nodes, Fig. 7).

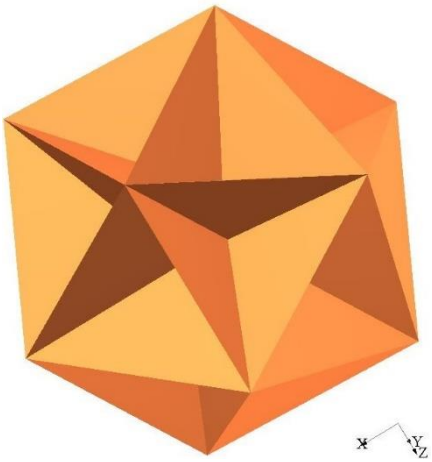

Fig.6. Icosahedron

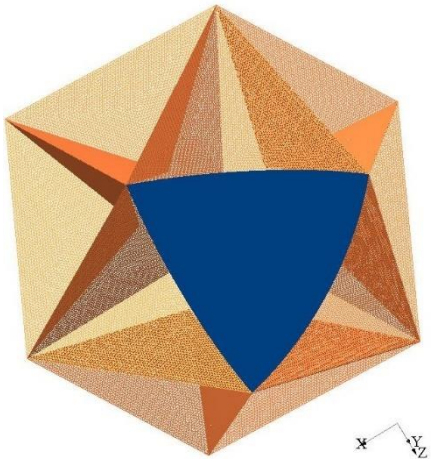

Fig.7. Observation surface (spherical part)

The "reference" solution (Fig. 8) was computed using a direct and iterative solver with a conventional BE method. The comparison with the result of the BEAM method (Fig. 9) only gives some minor differences in quieter areas (less than -15 dB, white dotted circles).

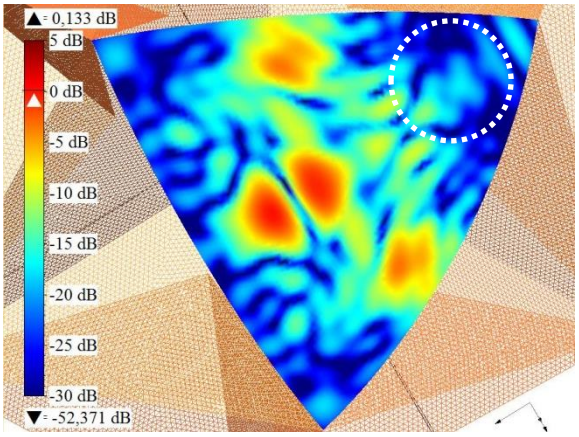

Direct solver, matrix-based (Intel MKL)

Δt_{solve}:	11,116	s (3:05:13 h)
s_{matrix}:	198,095	MB

Iterative solver, matrix-based (GMRES)

N_{iter}:	76	$e_{iter} = 8.8\times10^{-7}$
Δt_{solve}:	709	s

Fig.8. bistatic, BEM, matrix-based, *TS*, rigid, f = 100 kHz, Observation surface (spherical segment)

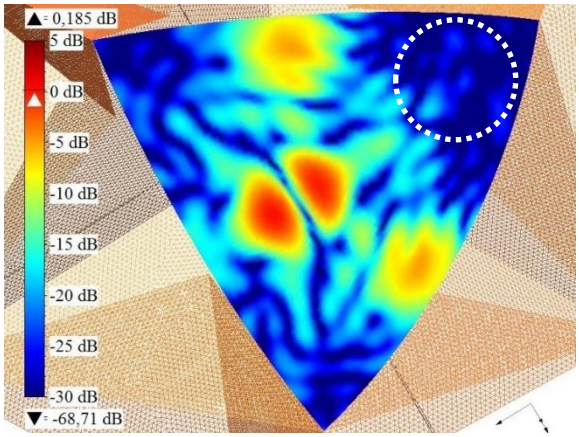

BEAM method

Δt_{solve}:	0.5	s
S_{beam}:	< 10	MB

Fig.9. bistatic, BEAM (raytracing), *TS*, rigid, f = 100 kHz, Observation surface (spherical segment)

3.5.2 Icosahedron (monostatic)

Here, a monostatic calculation was performed for all 4,360 nodes of the observation mesh (Fig. 11).Due to the fact that a direct solver is capable of using multiple right-hand sides, which results from changing the position of the sound source without refactorizing the underlying system matrix, a reference solution is also available(Fig. 10).

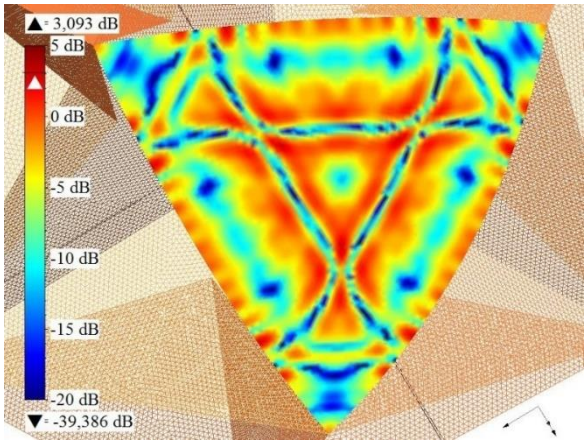

Direct solver, matrix-based (Intel MKL)
Δt_{solve}: 31,667 s (8:47:40 h)
s_{matrix}: 198,095 MB

Fig.10. monostatic, BEM, matrix-based, *TS*, rigid,*f* = 100 kHz, Observation surface (spherical segment)

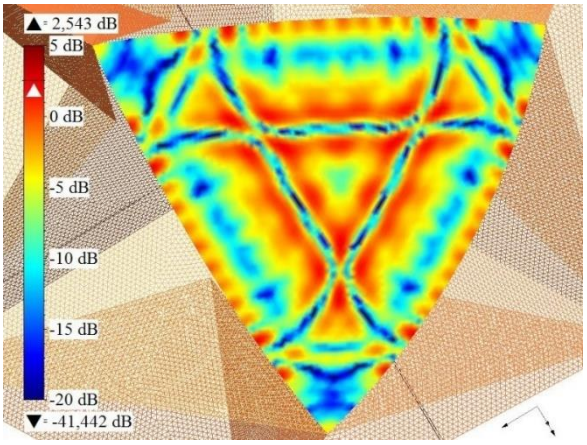

BEAM method
Δt_{solve}: 65.8 s
S_{beam}: < 10 MB

Fig.11. monostatic, BEAM, *TS*, rigid,*f* = 100 kHz, Observation surface (spherical segment)

3.5.3 Model 2 of BeTSSi workshop (monostatic)

To compare the results of different methods for shell-like structures, a rounded air-filled cylinder (for details, see [9]) was used; this had 4 triple mirrors at the left end and one triple mirror at the right end (approx. size 46 × 6 × 6m).The cylinder and the plates at the left end are modeled as a 20mm steel shell.

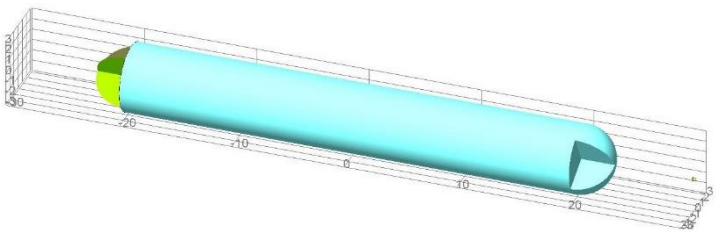

Fig.12. Model 2

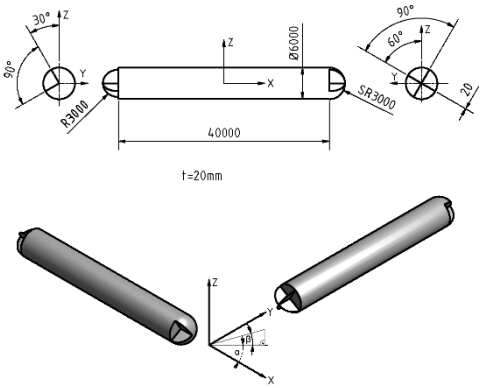

Fig.13. Dimensions and sizes of model 2

Fig. 14 shows the result (target strength) for this model at a frequency of *f* = 3kHz. Both solutions show satisfying accordance, but the solution time for the approximate raytracing solver is more than 300 times lower.

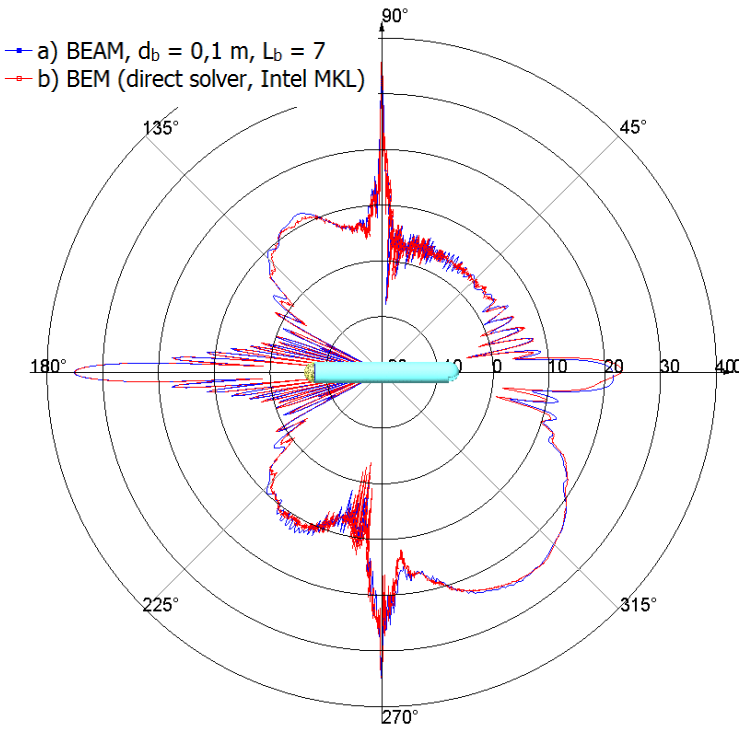

Monostatic calculation, rigid

f:	3	kHz
N_{elem}:	217,065	
N_{FP}:	720	
$\Delta\alpha_{STEP}$:	0.5°	
Calculation times:		
t_{IMKL}:	39,840	s (11:04:00)
t_{BEAM}:	146	s

Fig.14. Target strength of Model 2, f = 3 kHz.

3.5.4 Advanced capabilities

To illustrate the advanced capabilities of the raytracing-based BEAM method, a rounded cylinder is used with several triple mirrors on the caps. The cylinder is surrounded by a conical shell (Figure 15, approx. size 49 × 10 × 10m, details see [10]). The inner cylinder, filled with air, and the triple mirrors at the left end, are represented by steel with a thickness of 2cm. The outer conical hull is made of steel with a thickness of 8mm, filled with, and surrounded by, water.

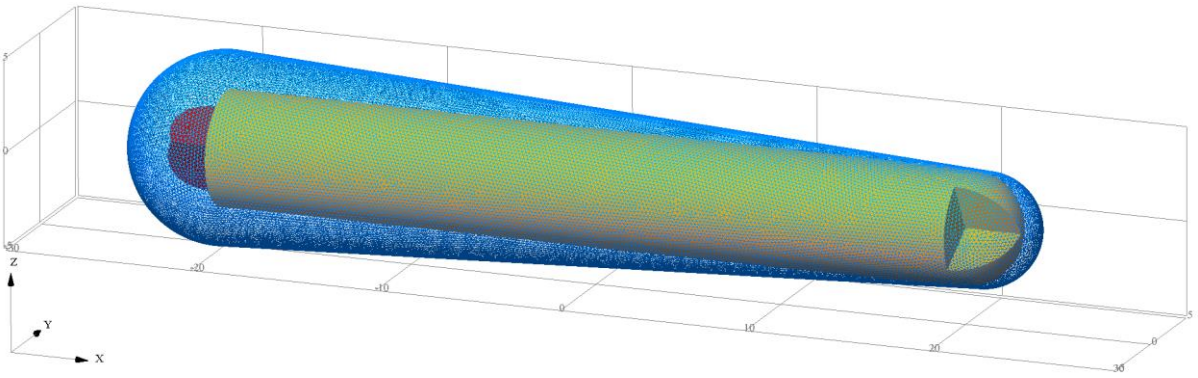

Fig.15. Complex model of a round cylinder with one resp. four triple mirrors at the ends, surrounded by a conical rounded shell.

A grid in the form of a spherical segment (longitude λ_L of -180 ... +180°, latitude φ_B of -20 ... +20°, using angular steps of 0.5°) is placed in the far-field at a distance of 10km around the object. Its nodes are used as evaluation points (total of 58,401 points) for a monostatic calculation. That means that the position of the sound source was moved to each evaluation point. For a better representation of the results, a projection distance of 30m is used (Fig. 16).

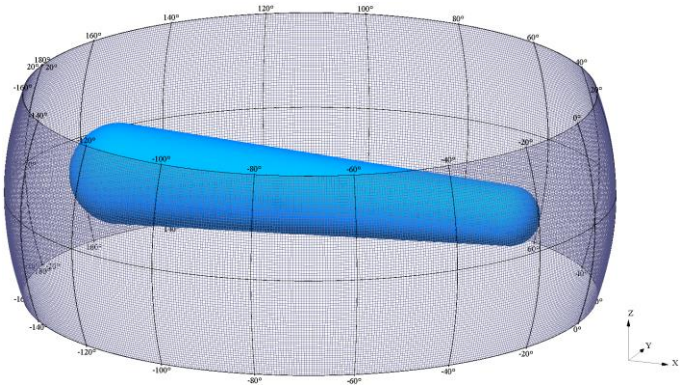

Fig.16. Spherical evaluation surface (58,401 nodes), using a projection distance of 30m.

The size and complexity of this model makes a monostatic calculation with BE or FE methods over a realistic time almost impossible, and is only feasible with the use of the BEAM method.

The target strength was calculated for a total of 21 frequencies (f = 8 ... 12 kHz, step width Δf = 0.1 kHz) for all of the 58,401 evaluation points, and in addition, an appropriate averaging process was carried out over all the frequencies used (Fig. 17).

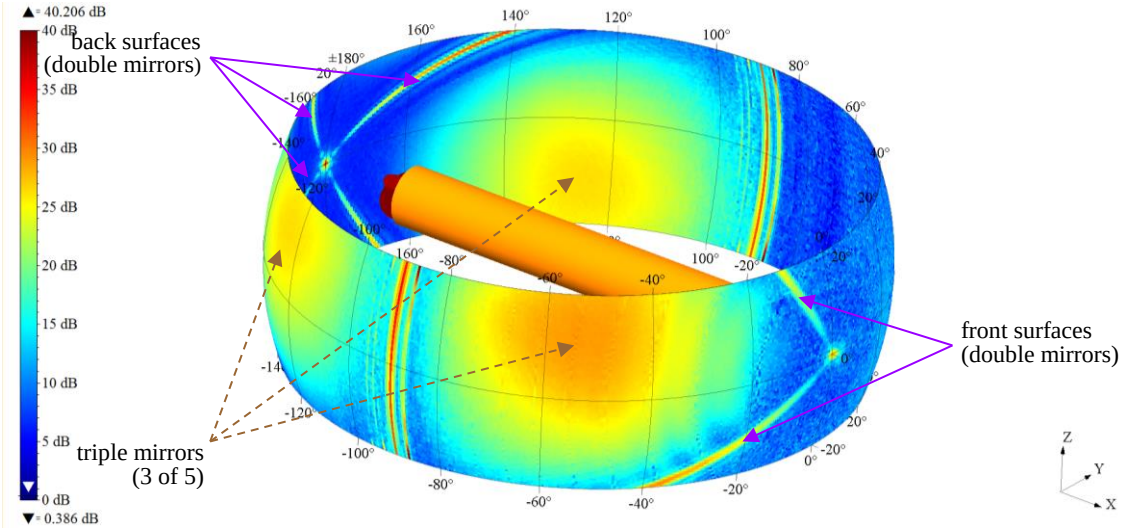

Fig.17. Averaged target strength TS for f_{aver} = 10 kHz.

One can clearly see the effects of the triple mirrors in the front and rear. The computation time for all 58,401 evaluation points s well as all 21 frequencies was about 6,976s on a 20 core workstation, which corresponds to a mean solving time of 0.119s per point.

REFERENCES

[1] H.G. Schneider, Rough boundary scattering in raytracing computations, Acoustica 35, p. 18, 1976.

[2] H.G. Schneider, Excess sound propagation loss in a stochastic environment, J. Acoust. Soc. Am., Vol. 62, 871-877, 1977.

[3] J. Sellschopp, Stochastic raytracing in thermoclines, In Ocean Variability and Acoustic Propagation, Potter and Warn-Varnas (ed.), Kluwer, 1991.

[4] R. Thiele, A comparative test of shallow water sound propagation models against real data, SACLANTCEN Report SR 149, La Spezia, Italy, 1989.
[5] F. Gerdes, H.G. Hofmann, I. Nissen, Comparison of measured and modeled acoustic propagation loss in the Baltic Sea, In Seventh European Conference on Underwater Acoustics, D.G. Simmons, pp 51-56, 2004.
[6] H.G. Hofmann, D. Brecht, F. Gerdes, Propagation loss modelling and measurements under conditions with high spatial variability, In UDT Europe, Naples, Italy, 2007.
[7] F. Gerdes, H.G. Hofmann, W. Jans, S. Künzel, I. Nissen,H. Dol, Measurements and simulations of acoustic propagation loss in the Baltic Sea, Proc. Underwater Acoustic Measurements: Technologies & Results,Papadakis (ed.), Greece, 2009.
[8] R. Burgschweiger, I. Schäfer, M. Ochmann, B. Nolte,BEAM: A ray-tracing based solver for theapproximate determination of acousticbackscattering of thin-walled objects -Basics and Implementation, Proceedings of Forum Acusticum, Krakow, Poland, 2014.
[9] B. Nolte, I. Schäfer, C. de Jong,L. Gilroy, BeTSSi II Benchmark on Target Strength Simulation, Proceedings of Forum Acusticum, Krakow, Poland, 2014.
[10] R. Burgschweiger, I. Schäfer, M. Ochmann, B. Nolte,Results of the ray-tracing based solver BEAM for the approximate determination of acoustic backscattering from thin-walled objects, Proceedings of the Inter-noise, Melbourne, Australia, 2014.